Bitlis Eren Üniversitesi Fen Bilimleri Dergisi
BİTLİS EREN UNIVERSITY JOURNAL OF SCIENCE
ISSN: 2147-3129/e-ISSN: 2147-3188
VOLUME: 11 NO: 3 PAGE: 861-879 YEAR: 2022
DOI: 10.17798/bitlisfen.1130044

A Comparison of Ensemble and Base Learner Algorithms for the Prediction of Machining Induced Residual Stresses in the Turning of Aerospace Materials

Selim BUYRUKOĞLU[1], Sinan KESRİKLIOĞLU[2*]

[1]*Department of Computer Engineering, Cankiri Karatekin University, Cankiri, Turkey*
[2]*Department of Mechanical Engineering, Abdullah Gul University, Kayseri, Turkey*
(ORCID: 0000-0001-7844-3168) (ORCID: 0000-0002-2914-808X)

Keywords: Residual Stress, Machining, Inconel, Titanium, AdaBoost, Neural Network.

Abstract

The estimation of residual stresses is essential to prevent the catastrophic failures of the components used in the aerospace industry. The objective of this work is to predict the machining induced residual stresses with bagging, boosting, and single-based machine learning models based on the design and cutting parameters used in the turning of Inconel 718 and Ti6Al4V alloys. Experimentally measured residual stress data of these two materials was compiled from the literature, including the surface material of the cutting tools, cooling conditions, rake angles, as well as the cutting speed, feed, and width of cut to show the robustness of the models. These variables were also grouped into different combinations to clearly show the contribution and necessity of each element. Various predictive models in machine learning (AdaBoost, Random Forest, Artificial Neural Network, K-Neighbors Regressor, Linear Regressor) were then applied to estimate the residual stresses on the machined surfaces for the classified groups using the generated data. It was found that the AdaBoost algorithm was able to predict the machining induced residual stresses with a mean absolute error of 18.1 MPa for the IN718 alloy and 31.3 MPa for Ti6Al4V by taking into account all the variables, while the artificial neural network provides the lowest mean absolute errors for the Ti6Al4V alloy. On the other hand, the linear regression model gives poor agreement with the experimental data. All the analyses showed that AdaBoost (boosting) ensemble learning and artificial neural network models can be used for the prediction of the machining induced residual stresses with the small datasets of the IN718 and Ti6Al4V materials.

1. Introduction

Titanium and nickel-based super alloys are widely used in aerospace applications due to their high specific strength, wear, corrosion, and oxidation resistance. Residual stresses are generated in machining due to the inhomogeneous plastic deformation and chip formation processes, and the interactions between the tool and freshly machined surface. The low thermal conductivity of these workpiece materials increases the temperature at the cutting edge of the tool and changes the shape and strength of the parts due to the thermally induced tensile residual stresses. Moreover, the high strength of these super alloys reduces the machinability and increases the cutting and thrust forces during machining, which results in an increase in the level of the comprehensive residual stresses. Since aerospace components are exposed to excessive loads and temperatures due to their critical roles and operations, the thermomechanical residual stresses on the machined surface significantly influence the fatigue life and lead to catastrophic failures of airframes and engine parts. Residual stress is thus one of the most important parameters in evaluating the quality of the machined parts, and eliminating or minimizing the

*Corresponding author: sinan.kesriklioglu@agu.edu.tr
Received: 13.06.2022, Accepted: 01.09.2022

detrimental effects of it with the optimum cutting condition and tool setup is critical to ensure the surface integrity of the aeronautical components [1].

Due to the high usage of these alloys, extensive research and techniques have been conducted to improve the machining characteristics and part quality. The effect of cutting parameters (cutting speed, feed, and width/depth of cut) on the residual stresses was investigated in the machining of Inconel 718 and Ti6Al4V alloys. Holmberg et al. [2] performed cutting experiments and particle finite element simulations to investigate the effect of cutting parameters on the machining induced residual stresses in the orthogonal turning of Ti6Al4V. It was found that the surface residual stresses were tensile in the cutting direction and directly proportional to the feed while high compressive residual stresses were observed at the lowest cutting speed for the cutting conditions tested in the study. The tendency regarding the feed was also similar when cutting Inconel 718 [3], but the mode of residual stress did not change with the cutting speed. The residual stresses induced in the turning of Inconel 718 were also experimentally measured to optimize the cutting parameters for minimum residual stresses through a general algorithm function [4]. Another optimization process was carried out in the turning of Inconel 718 with a coated cutting tool [5]. The cutting tests were designed with the Grey Taguchi method and an ANOVA analysis was performed to investigate the contribution of cutting parameters to the surface residual stresses. It was found that the feed had a significant effect on the residual stress while maximizing the material removal rate, and it was followed by the depth of cut and cutting speed. The contribution of the feed was also similar to the machining of Ti6Al4V [6]. However, increasing the depth of cut result in deeper residual stresses [7].

The influence of the cooling condition, cutting tool material, and rake angle on the magnitude of the surface residual stresses has also been reported in many research papers. It was found that these parameters significantly affect the magnitude and modes (tensile and compressive) of the surface residual stresses induced during the machining operations. Ayed et al. [8] employed cryogenic cooling at various flow rates and pressures in the machining of Ti6Al4V and compared its effectiveness in reducing the surface residual stresses under conventional cooling and dry cutting. Cutting tests showed that cryogenic cooling at the highest flow rate and pressure produced the greatest compressive residual stresses although it reduces the thermal loads in the machining of Ti6Al4V. The impact of flood cooling on the residual stresses induced during the machining of Inconel 718 was also investigated with a coated carbide tool [9]. It was found that the magnitude of tensile residual stresses with the highest cutting speed was similar for dry and flood cooling. The effect of rake angle on the surface residual stresses was studied on the Ti6Al4V thin walls manufactured by selective laser melting. Turning experiments were conducted with zero and positive rake angles besides the various tool nose radius and cutting parameters [10]. It was found that the rake angle and tool nose radiuses influenced the magnitude of the compressive surface residual stresses in both cutting and feed directions. Three-dimensional finite element simulations were also performed to investigate the effect of tool coating on the residual stresses induced during the turning of Ti6Al4V and the results were validated by the experiments [11]. It was concluded that TiAlN coated tools increased the tensile residual stresses on the machined surfaces when compared to the uncoated tungsten carbide tools, although the cutting edge radius of the coated tool was larger than the uncoated tools. However, the residual stresses were more compressive with multilayered cutting tools in a different study [12]. The surface residual stresses also became more tensile with the coated cutting tools in the machining of Inconel 718 [13]. This could be due to the greater heat input into the workpiece materials since the coating provides a thermal barrier to the cutting tool. Simeone et al. [14] studied the influence of cooling on the surface residual stresses in the turning of Inconel 718. The experiments showed that the surface residual stresses were slightly lower under dry conditions with severe cutting conditions.

X-Ray diffraction is used to experimentally measure the surface residual stresses induced during the machining operations [15]. However, this method is expensive and time-consuming, and cannot be used for all combinations of the cutting parameters and tool setup. Therefore, it has been mostly used in the validation of analytical and numerical models. Analytical approaches are also used to calculate the machining induced residual stresses in a variety of materials. An analytical model was developed to predict the residual stresses in the orthogonal turning of AISI 4340 steel [16]. Two different algorithms were used because the hybrid algorithm provided a closer agreement with the experimental measurements than the S-J algorithm at low feed rates. A thermo-mechanical model incorporating the properties of workpiece material and cutting conditions was proposed to estimate the surface residual stresses in orthogonal machining [17]. The predicted and experimental results showed that this model can closely capture the trends of the residual

stress for AISI 316L and 4340 steel alloys. An analytical elasto-plastic model was also employed to obtain the residual stress profiles in the surface and subsurface layers of machined parts [18]. The magnitude and trend of residual stresses were able to be predicted within a short time. However, despite these strengths of analytical models, simplifying assumptions make them difficult to apply for all types of alloys due to the different strain hardening tendencies and toughness during the deformation of the workpiece materials (i.e., turning).

Advances in computer technology have increased the use of numerical models in simulating the machining process. Finite element models were combined with constitutive material models to predict the temperature and stress distribution on the workpiece and cutting tool during and/or after the machining process when all the thermal and mechanical loads are removed. A commercially available three-dimensional finite element model was used with a Lagrangian implicit code to predict the machining induced residual stresses in the turning of Inconel 718 and AISI 316L steel [19]. Finite element simulations showed that regardless of the tool material, the mode of the machining residual stresses was tensile at surface, but it gradually became compressive beneath the machined the surface for Inconel 718. Sahu and Andhare [20] used a similar finite element approach to simulate the turning operation of Ti6Al4V at various cutting conditions. ANOVA analysis was performed to optimize the cutting parameters since the model was able to predict the residual stresses with a mean absolute error of 11%. An implicit two-dimensional plane-strain finite element model [21] was developed to estimate the residual stresses in the turning of Inconel 718 turbine disks, and the proposed model was validated with the experimental measurements and analytical models published in the literature. The predicted values of the finite element model match better with the analytical model by assuming the rigid-plastic constitutive law. Although the numerical simulations provide close agreement with the experimental data in depth profiles when applying the appropriate material models, the magnitude of the residual stresses on the machined surfaces significantly deviates due to the relatively coarse mesh size, which is required to reduce the computation time.

With the impact of artificial intelligence in engineering applications, machine learning-based approaches have become more narrowly applied to predict the surface residual stresses in the literature. In a study, the effect of the machining parameters on the machining induced residual stresses was investigated by employing Artificial Neural Network (ANN) and Genetic Algorithm (GA) [4]. ANN was also used in different research to predict the value of surface residual stresses in the face turning operation [22]. Moreover, the ANN approach was used in the assessment of axial and hoop subsurface residual stresses in the hard turning of 52100 bearing steel [23], and the predicted results under various cutting speeds and feeds were validated with numerical and experimental data. Since only cutting speed, feed rate, and depth of cut were used as input parameters to predict the residual stress with these algorithms for the machining of Inconel 718, this research does not provide insights into the prediction accuracy when using different experimental setups (i.e., machining with coated inserts under flood cooling). The Gaussian Process Regression was also implemented to estimate the surface residual stresses in end milling [24]. A random forest was initially employed to determine the optimum feature set. Then, Gaussian Process Regression, Support Vector Regressor, ANN, and AdaBoost algorithms were employed to predict surface residual stress in end milling. The best prediction performance was obtained through the Gaussian Process Regression. Since all the residual stresses are measured using the same conditions for X-Ray diffraction, the performance of the models was not evaluated for the existence of the uncertainties in the X-Ray measurements. ANN and fuzzy neural network models were compared to highlight the prediction performance of the models for the residual stresses in the welding operation. The fuzzy neural network model provided slightly better performance in the prediction process with the root mean square error (RMSE) of 0.12, R-squared (R2) of 0.91, and mean absolute percentage error (MAPE) of 22.94 compared to the ANN [25]. The ANN technique has also been adapted to predict and optimize the surface residual stresses induced by the laser shock peening process on a Ti6Al4V alloy [26]. The ANN predictions were in good agreement with the experimental results.

Even if all the aforementioned studies were accomplished to obtain promising results, to the best of the authors' knowledge, bagging and boosting ensemble machine learning models have never been used for the prediction of surface residual stresses in the turning operation. Thus, the objective of this work is to predict the residual stresses with the machine learning models in the turning of Inconel 718 and Ti6Al4V alloys. The machining induced residual stress data were extracted from the experimental studies in the literature since performing the cutting experiments on these aerospace materials, and measuring the residual stresses by X-Ray diffraction are expensive., This type of data collection process

also enables us to implement the machine learning models for all the combinations of cutting and design parameters, and a relatively small number of the datasets (i.e., machining induced residual stress). Since most of the researchers concluded that single-based models may perform better than ensemble learning algorithms including bagging and boosting for the regression and classification cases [27], [28], popular single-based models (k- Nearest Neighbors, Naive Bayes, Support Vector Machine, Linear Regression, and Artificial Neural Network) were selected in addition to the ensemble learning algorithms based on the efficiency of the regression problems in different fields. Then, the effectiveness of these models was evaluated based on the R2 value. This statistical metric was also used to determine the optimal bagging and boosting algorithms, including Random Forest and AdaBoost. This paper is also motivated by the comparisons of the bagging (Random Forest) and boosting (AdaBoost) algorithms in terms of prediction accuracy. Additionally, single-based models (Linear Regression, K-Nearest Neighbor, and ANN) were employed to compare the single-based models with the bagging and boosting ensemble machine learning models.

2. Methodology

A brief description of the turning operation is given in this section. The machining terminology used in the datasets and data collection process is explained. The machine learning models to predict the machining induced surface residual stresses in turning of Inconel 718 and Ti6Al4V alloys are also presented. In addition, the metrics are expressed to evaluate the accuracy of the models in estimating the experimentally measured residual stresses.

2.1. Turning Operation

Turning is a material removal process carried out on a CNC or engine lathe to obtain perfect inner and outer cylindrical and/or conical surfaces as well as external and internal threads. In this process, the workpiece rotates at high speeds, and stationary cutting tools, which are made of a much harder material than the workpiece, plastically deform the material to the desired dimensions and shapes. Figure 1 illustrates the schematic representation of the turning operation. A coating is generally required to reduce the friction between the cutting tool and workpiece and increase the wear, oxidation, fatigue, and thermal shock resistance that extend the tool life significantly. High material removal rates are also desired in machining operations to increase process productivity. Cutting speed, feed, and depth/width of cut determine the volume of the material that is being cut. Cutting speed is defined as the rotational or surface speed of the workpiece and is usually expressed in revolution per minute or meter per minute, respectively. Feed is defined as the distance that the cutting tools travel for each revolution of the workpiece, while the depth/width of cut is the distance measured from the surface of the workpiece material to the tool tip, and expressed in millimeters. Since these variables are directly proportional to the material removal rate, increasing them produces higher efficiency in the machining process. However, excessive increases in the speed, feed, and depth of cut accelerate the tool wear due to high cutting forces and temperatures and result in poor surface finishes. Therefore, optimization of the cutting parameters is required with respect to the surface integrity of the workpiece and machining costs in order to efficiently achieve the turning operation of aerospace materials.

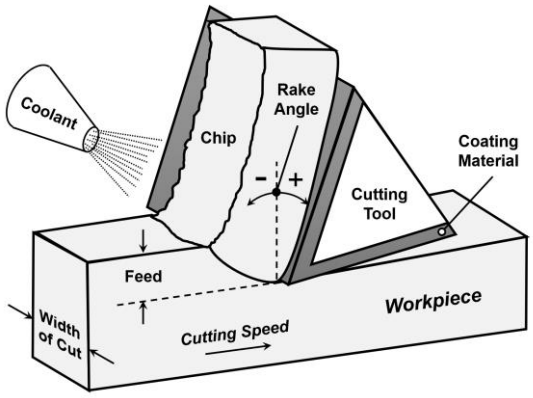

Figure 1. Schematic illustration of turning process

The rake angle is another tool setup parameter that describes the angle of the cutting tool face relative to the workpiece surface, as shown in Figure 1, and it significantly influences the residual stresses in turning since it changes the formation of chip and shear flow. It should be noted that the rake angle is classified as positive, negative, and zero in the data sets of this paper because an adequate sample size could not be found in the literature to numerically show its contribution to the surface residual stresses. Although dry cutting can be the most sustainable option in the machining operation, active cooling is also implemented to reduce the temperature, oxidation, and tool wear in the turning of nickel and titanium alloys. A synthetic water-based metal working fluid (MWF) is commonly used to flood the machining zone for cooling and lubricating the cutting tool while the minimum quantity lubrication (MQL) technique and cryogenic machining (CRYO)

with liquid nitrogen can be considered as alternatives to satisfy the environmental concerns.

2.2. Data Collection

Due to the high cost of the experiments for all possible combinations, the effects of tool material, rake angle, cooling condition, cutting speed, feed, and width of cut on the machining induced surface residual stresses were obtained from the literature and tabulated in Appendix 1 and 2 for the Inconel 718 and Ti6Al4V alloys, respectively. Two different commonly used and commercial aerospace materials were selected to show the robustness of the machine models described in the subsequent section and that the methodology can be extended to other types of materials and machining setups. Only experimentally measured residual stresses by the X-Ray Diffraction technique were compiled from the literature to validate the machine learning models with high confidence.

The datasets used in this study include six independent variables based on the machining setup and cutting parameters. Some of them may play a key role in the prediction of machining induced surface residual stress. Thus, five different groups were created from the entire datasets and then the performances of the machine learning models were compared to reveal the importance of the variables on the prediction of surface residual stress based on the existing data. Table 1 lists all the groups created to clearly show the contribution of the variables to the machining induced residual stresses for aerospace materials.

Table 1. Created groups from the entire residual stress datasets

Group #	Group Name
1	All variables
2	Only cutting parameters (cutting speed, feed and width of cut)
3	Cutting parameters and tool material
4	Cutting parameters and coolant
5	Cutting parameters, tool material and coolant (rake angle is excluded)

2.3. Modelling

Various machine learning models were applied to determine the correct model for the prediction of the surface residual stresses in the turning of aerospace materials. The Decision Tree, k- Nearest Neighbors, Random Forest, AdaBoost, Naive Bayes, Support Vector Machine, Linear Regression, and Artificial Neural Network were first tested and five of the machine learning models were selected based on the r-squared values (R2). AdaBoost, Artificial Neural Network, Random Forest, k-Nearest Neighbors, and Linear Regression were found the best models for the datasets of the Inconel 718 and Ti6Al4V alloys given in Appendix 1 and 2. Each dataset was then separated into training (80%) and test (20%) sets, and 10-fold cross-validation was used in the training set. Finally, models were evaluated based on the test set. In other words, nested cross-validation was used in the training and evaluation process of the machine learning models [29]. Figure 2 shows the flow diagram of the residual stress prediction system used in this study.

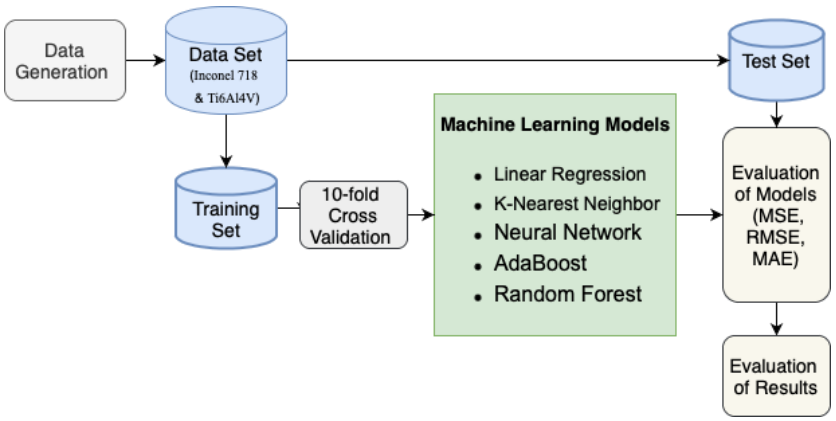

Figure 2. Flow diagram of residual stresses prediction system

AdaBoost

AdaBoost is a type of boosting ensemble algorithm, which was initially proposed by Freund and Schapire [30]. The core principle of it is to combine weak learners for the generation of a strong algorithm. In the working process of the AdaBoost algorithm, a simple learning algorithm is called at each iteration, and then a weight coefficient is assigned to this learning algorithm. The assigned weight coefficient is inversely proportional to the simple learning algorithm's error. In the end, this model provides a solution based on the weighted voting. Even though the AdaBoost algorithm was proposed to solve the classification problems, Drucker adapted it to solve regression problems [31]. The modified version of the algorithms is known as AdaBoost.R2 in the literature. In this study, 100 estimators (decision stumps) were used in the employed AdaBoost.R2 algorithm.

Linear Regression

Simple and multiple linear regressions are mostly used for regression problems in the literature. Single linear regression mostly provides convincing results when the output is predicted using a single predictor. On the other hand, multiple linear regression generally allows for obtaining more effective results if the output is obtained using more than one predictor [32]. A random relationship among variables is created based on the present data to obtain statistical relations. In this study, machining induced residual stresses in the turning of aerospace materials were predicted with more than one predictor, and multiple linear regression can, thus, be employed.

Artificial Neural Network

Artificial neural networks (ANN) are widely used as predictive modeling in different disciplines. The structure of the ANN consists of three layers including the input, hidden, and output layers. Many researchers specified that ANN models are employed with a single hidden layer, giving convincing results and shortening the prediction process. The hidden layer neuron variations were used to determine the optimal number of neurons for a hidden layer [33]. Additionally, a hidden layer with 12 neurons was used in the creation of an ANN structure [34]. It can be inferred from these studies; researchers tend to obtain convincing statistical scores using a variety of neurons in a single hidden layer. Therefore, a single hidden layer was used in the proposed ANN model. In order to determine the optimum number of neurons in the hidden layer, various values were used in the creation process of the ANN model. It is also stated that the number of neurons used in the hidden layer should not be more than twice numbers of neurons in the input layer [35], [36]. Therefore, 3, 6, 9, and 12 neurons were used in the hidden layer, and the ANN model was achieved to provide the best performance through the 6 neurons. Additionally, the maximum number of iterations was set to 300 as a result of trying different values such as 50, 150, 300, and 500. ReLu was used as an activation function while Adam optimization was used as the training algorithm in the employed ANN model. The proposed ANN is, thus, created with the following parameters: a single hidden layer with 6 neurons, number of iterations is 300, activation function was ReLu, and the solver is Adam optimization. Also, the ANN structure is determined for both datasets due to the similar sample sizes. Dataset 1(Datasets of Inconel 718) consists of 97 samples. Dataset 2 (Datasets of Ti6Al4V) consists of 91 samples. Figure 3 presents the structure of the proposed ANN model used in this study.

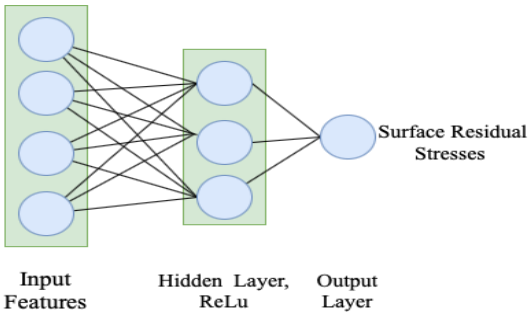

Figure 3. Structure of the employed ANN model

K-Nearest Neighbor (kNN)

The kNN algorithm aims to keep similar things close to each other. Different metrics can be used in order to find close similar things in the creation of a kNN model (i.e. Euclidean, Manhattan, Chebyshev, etc). The K-Neighbors Regressor algorithm was also applied to predict surface residual stress in the turning of Inconel 718 and Ti6Al4V. In the regression problems, the mean of the numerical target of the k nearest neighbors is calculated, and the K-Neighbors Regressor uses the same distance measured as the kNN classification [37]. In this study, the Euclidean criterion was used while calculating the distance values between samples, and the number of neighbors was set to 5, as the default value for the number of neighbors in sklearn is 5.

Random Forest

The Random Forest is a type of ensemble (bagging) algorithm which is an extension of the decision tree. If a model consists of more than one decision tree, it is considered a random forest. In the Random Forest model, the Bootstrap sampling method is used to extract multiple samples from the original samples. Then, decision trees are combined for the prediction. An average estimate is taken from the decision trees used in the random forest to obtain the prediction result [38]. In this study, the number of trees was set to 100, and subsets were not spilt when they were less than 5.

Evaluation Metrics

Mean Squared Error (MSE), Root Mean Square Error (RMSE), Mean Absolute Error (MAE) and R-Squared (R2) are effective evaluation metrics in terms of interpretation of the prediction models [39]. These metrics are calculated as

$$MSE = \frac{1}{n}\sum_{i=1}^{n}\left(P_i - \hat{P}_i\right)^2 \quad (1)$$

$$RMSE = \sqrt{\frac{1}{n}\sum_{i=1}^{n}\left(P_i - \hat{P}_i\right)^2} \quad (2)$$

$$MAE = \frac{1}{n}\sum_{i=1}^{n}\left|P_i - \hat{P}_i\right| \quad (3)$$

$$R^2 = 1 - \frac{RSS}{TSS} \quad (4)$$

where P_i is the actual value, $\hat{P}_i$ is the predicted value from the model, n is the number of observations, RSS is sum of squares of residuals and TSS is total sum of squares.

3. Results and Discussion

This section presents the experimentally measured residual stresses by X-Ray Diffraction in the turning of Inconel 718 and Ti6Al4V alloys and predicted results by the machine learning models described in the previous section. It should be noted that the experimentally measured residual stresses were combined from a variety of research papers focusing on the experimental studies as highlighted in the previous section. However, the experimental measurements by X-Ray Diffraction still include uncertainties [40] and they could be considered an outlier due to the high margin of error in the measurement. Thus, the Mean Absolute Error (MAE) values of the models were mainly used in this paper to evaluate the employed models' efficiency since the Mean Squared Error and Root Mean Squared Error are more sensitive to outliers than the MAE, and R2 is less robust to outliers than the MAE [41]. Moreover, ensemble and some of the single-based algorithms are flexible algorithms (neural network, AdaBoost, Random Forest, etc.) compared to the statistical models (Linear Regression, etc.). In this sense, flexible algorithms usually provide convincing results even if the dataset contains outliers [42].

3.1. The Comparison of Experimental and Predicted Machining Induced Residual Stresses for Inconel 718

The effect of machining variables on the performance of machine learning models for the prediction accuracy of residual stresses in the turning of Inconel 718is presented in Table 2 based on the test scores. The employed AdaBoost algorithm provides the best performance in all data groups with respect to all the metrics used in this study when compared to the other machine learning algorithms. In contrast to the AdaBoost algorithm, Linear Regression has the worst MSE, RMSE and R2 values in the prediction of machining induced residual stresses for Inconel 718. The lowest MAE value (14.9) was obtained with the AdaBoost algorithm when the rake angle is excluded (Group 5). Moreover, the AdaBoost algorithm achieved to obtain an MAE value of 18.1 when all variables are used in the predicted models. In this sense, the efficiency of the Rake Angle can be considered the lowest among the other variables. On the other hand, the AdaBoost algorithm gives the worst MAE value (50.7) when only the cutting parameters (Group 2) are taken into the account in the predictions. When Groups 3 and 4 are used in the prediction process, the performance of the AdaBoost algorithm is higher than the ones with Group 2. However, this algorithm has provided slightly better performance when Group 4 is used in the prediction process as compared to the algorithm performance when Group 3 is used. It means that the cooling can be considered a more effective variable than the tool material type for the machining induced residual stresses of the Inconel 718. Moreover, the best MSE, RMSE, and MAE values in the AdaBoost and ANN models are obtained with Group 5 in which the rake angle data are excluded in the dataset of the prediction process[42].

Table 2. .The effect of the variable existence on the prediction accuracy of residual stresses in the turning of Inconel 718

Group 1 (All variables)				
Model	**MSE**	**RMSE**	**MAE**	**R^2**
AdaBoost	2778	52.7	18.1	0.980
Linear Regression	44334	210.6	152.5	0.677
Neural Network	2995	54.7	29.3	0.978
K-Nearest Neighbor	42843	207.0	140.4	0.688
Random Forest	28490	168.8	128.1	0.792
Group 2 (Only Cutting Parameters)				
Model	**MSE**	**RMSE**	**MAE**	**R^2**
AdaBoost	14133	118.9	50.7	0.897
Linear Regression	73374	270.9	201.3	0.465
Neural Network	26099	161.6	113.3	0.810
K-Nearest Neighbor	51370	226.7	158.5	0.626
Random Forest	31011	176.1	136.1	0.774
Group 3 (Cutting Parameters and Tool Material)				
Model	**MSE**	**RMSE**	**MAE**	**R^2**
AdaBoost	7892	88.8	32.3	0.940
Linear Regression	70788	266.1	201.8	0.480
Neural Network	11050	105.1	61.5	0.920
K-Nearest Neighbor	41450	203.6	136.7	0.700
Random Forest	29801	172.6	130.3	0.780
Group 4 (Cutting Parameters and Coolant)				
Model	**MSE**	**RMSE**	**MAE**	**R^2**
AdaBoost	6754	82.2	32.1	0.950
Linear Regression	73310	270.8	202.9	0.470
Neural Network	12174	110.3	66.6	0.910
K-Nearest Neighbor	54681	233.8	151.5	0.600
Random Forest	30494	174.6	134.9	0.780
Group 5 (Cutting Parameters, Tool Material and Coolant)				
Model	**MSE**	**RMSE**	**MAE**	**R^2**
AdaBoost	1668	40.8	14.9	0.960
Linear Regression	65877	256.7	198.7	0.520
Neural Network	2207	47.0	21.8	0.950
K-Nearest Neighbor	41956	204.8	140.2	0.690
Random Forest	28511	168.9	128.7	0.790

As can be seen from Table 2 and Figure 4, the boosting ensemble learning model (AdaBoost) has a better performance when compared to the bagging ensemble learning model (Random Forest) and single-based models (Artificial Neural Network (ANN), Linear Regression, K-Nearest Neighbor) in the prediction of the surface residual stresses in turning of Inconel 718 alloy. The AdaBoost and ANN can almost exactly estimate 82% of the experimental results. The maximum errors of the AdaBoost and ANN models are 22% and 52% in the test data when all variables are used in the models. On the other hand, ANN has the second-best performance for these five data, and this model achieved the best MAE value (21.8) using Group 5 (Table 2). Generally, the ANN single-based model can be considered better than the bagging (random forest) ensemble learning model in the prediction of surface residual stresses for Inconel 718.

As explained in the section on the data collection process, the datasets were collected from various experimental studies. Thus, in Figures 4-7, the horizontal axis numbers refer to the numbers of each study, and each grid shows the residual stresses from one paper. For instance, the data number between 1 and 10 refers to data obtained from a study while the data number between 30 and 62 refers to data obtained from a different study in Figures 4 and 5. The range of the data for each study is also available in Appendix 1 and 2.

As shown in Figure 4 and 5, the highest difference between the experimental and predicted data points was observed with the Linear Regression. This could be because of the relationship between the mean of the variables (independent and dependent) since the mean is not a complete description of a variable and it is a limitation of this model [43]. On the other hand, although the k-Nearest Neighbor shows better performance than the Linear Regression, the deviations between the experimental and predicted residual stresses are not in an acceptable range for turning of Inconel 718 alloy since it is used in the aerospace industry to manufacture vital parts.

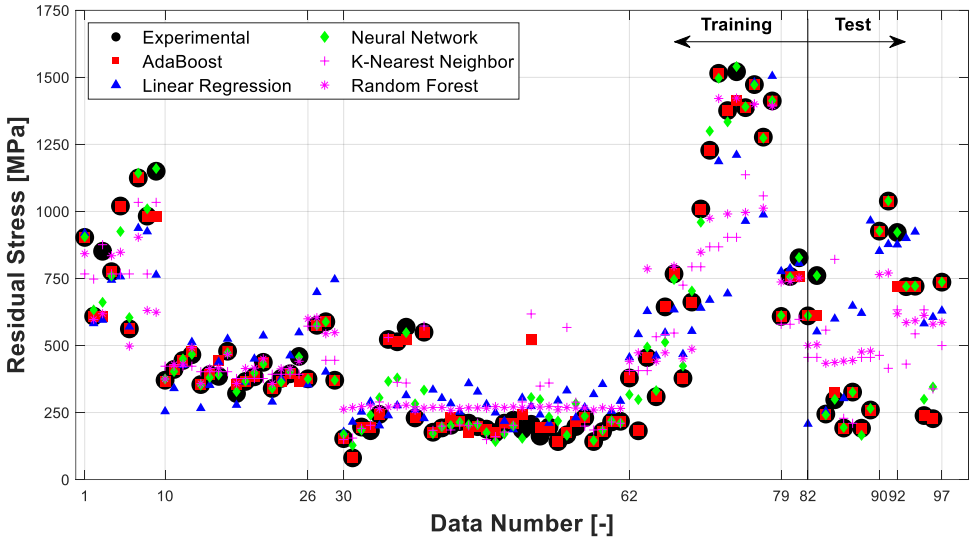

Figure 4. Experimental and predicted residual stresses in the turning of Inconel 718 with all variables

As shown in Figure 5, although the machine learning models are trained precisely, the agreement between the experimental and predicted residual stresses is poor in all the models when only the cutting parameters are used. This means that the information about the machining setup is required to obtain a reasonable residual stress prediction in the turning of Inconel 718. It also confirms that the machine learning algorithms used with only the various cutting parameters [4], [22], [24] do not completely provide the magnitude of the machining induced residual stresses. However, the AdaBoost could still capture 38% of the experimental results with a maximum error of 1% within the test data while the maximum error can be as large as approximately 200% in the AdaBoost and ANN machine learning models.

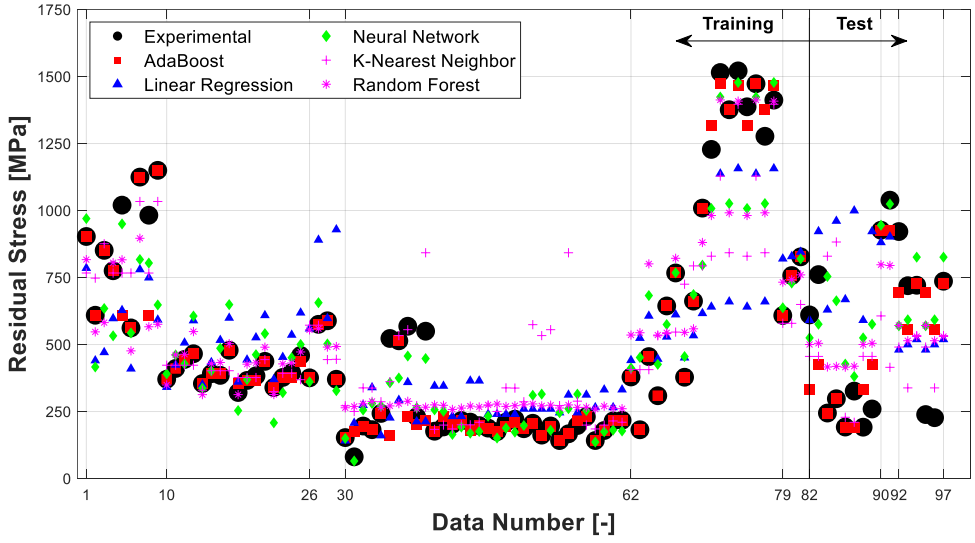

Figure 5. Experimental and predicted residual stresses in turning of Inconel 718 with only cutting parameters

3.2. The Comparison of Experimental and Predicted Machining Induced Residual Stresses for Ti6Al4V

Table 3 shows the effect of the variable contribution on the prediction accuracy of residual stresses in the turning of Ti6Al4V based on the test scores. As it can be seen from Table 3, the Artificial Neural Network (ANN) algorithm has the best performance for all the groups created in this study with respect to the MAE value. This algorithm has achieved providing the same and best MAE values (22.4) using Groups 1 and 5. On the other hand, although the AdaBoost algorithm seems to be the second-best model for the prediction of surface residual stress in the turning of Ti6aI4V, the difference between ANN and AdaBoost is only 0.2 when Group 2 is used in the analysis. In general, the ANN single-based model has better performance compared to the boosting and bagging learning algorithms for the prediction of surface residual stress in the turning of Ti6Al4V. Neural Network has the best MSE, RMSE, and R2 values compared to the other models, as shown in Table 3. The best values of MSE, RMSE, and R2 were obtained using Groups 1 and 5. In contrast to the Neural Network, Linear Regression provided the worst MSE, RMSE, and R2 values among the models presented in Table 3 due to the limitations of the linear regression mentioned in the previous section.

As can be seen from Figure 6 and 7, the AdaBoost and Neural Network algorithms show excellent prediction performance in the range from 86 to 91. However, these two algorithms provide the worst performance in the data numbered between 21 and 33 compared to the other experimental studies as shown in Figure 6. It can be seen in Appendix 2, that the effects of tool material and cooling conditions on the machining induced residual stresses were investigated in the work numbered between 21 and 33 [12]. Since the tool material and cooling type do not significantly influence the prediction accuracy of the machine learning models for the Ti6Al4V alloy (Table 3), these variables can be considered neutral elements in the prediction of machining induced residual stresses.

Table 3. The effect of the variable existence on the prediction accuracy of residual stresses in the turning of Ti6Al4V

Group 1 (All variables)				
Model	**MSE**	**RMSE**	**MAE**	**R^2**
AdaBoost	4364	66.1	31.3	0.960
Linear Regression	68535	261.8	183.6	0.365
Neural Network	1419	37.7	22.4	0.987
K-Nearest Neighbor	53008	230.2	152.8	0.509
Random Forest	40261	200.7	140.8	0.627
Group 2 (Only Cutting Parameters)				
Model	**MSE**	**RMSE**	**MAE**	**R^2**
AdaBoost	15104	122.9	55.9	0.860
Linear Regression	95676	309.3	243.6	0.114
Neural Network	9368	96.8	55.7	0.913
K-Nearest Neighbor	59377	243.7	171.6	0.450
Random Forest	43529	208.6	147.0	0.597
Group 3 (Cutting Parameters and Tool Material)				
Model	**MSE**	**RMSE**	**MAE**	**R^2**
AdaBoost	3967	63.0	33.0	0.963
Linear Regression	74155	272.3	200.0	0.313
Neural Network	2234	47.3	28.7	0.979
K-Nearest Neighbor	52275	228.6	151.7	0.516
Random Forest	41113	202.8	142.9	0.619
Group 4 (Cutting Parameters and Coolant)				
Model	**MSE**	**RMSE**	**MAE**	**R^2**
AdaBoost	4364	66.1	34.7	0.960
Linear Regression	81128	284.8	204.0	0.249
Neural Network	1578	39.7	24.7	0.985
K-Nearest Neighbor	54302	233.0	153.2	0.497
Random Forest	41500	203.7	143.8	0.616
Group 5 (Cutting Parameters, Tool Material and Coolant)				
Model	**MSE**	**RMSE**	**MAE**	**R^2**
AdaBoost	4364	66.1	31.3	0.960
Linear Regression	68535	261.8	183.6	0.365
Neural Network	1419	37.7	22.4	0.987
K-Nearest Neighbor	53008	230.2	152.8	0.509
Random Forest	40521	201.3	140.2	0.625

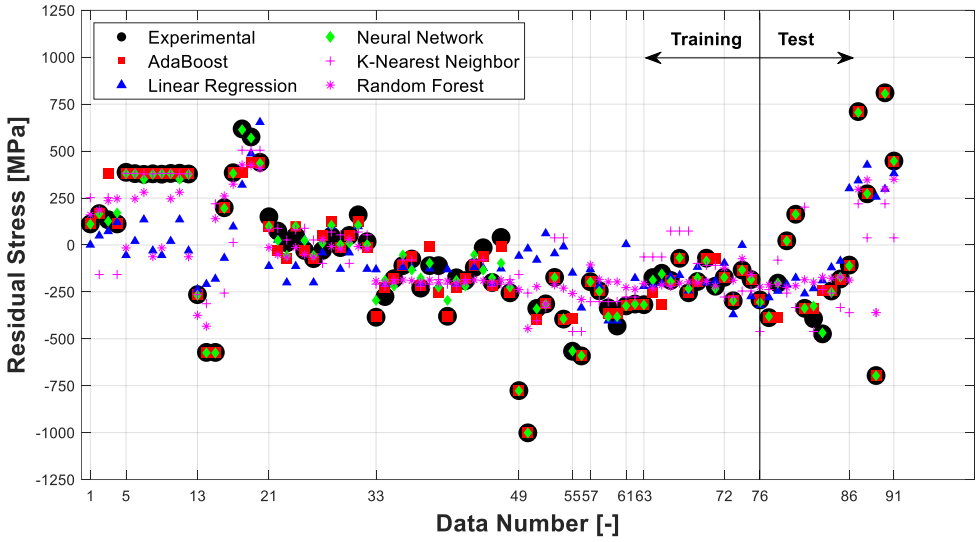

Figure 6. Experimental and predicted residual stresses in the turning of Ti6Al4V with all variables

As shown in Figure 7, each algorithm provided the same results for the samples numbered from 21 – 33 and 57 - 61. When the values of the cutting parameters (cutting speed, feed, width of cut) of these studies are checked in Appendix 2, they have the same values for each sample. Thus, the samples numbered between 21 and 33, 57 and 61 can be considered outliers in the dataset of Group 2. On the other hand, Linear Regression and Random Forest algorithms give similar results for the samples numbered between 33 and 49 while the experimental results and predicted values with the other employed algorithms are different (Figure 7). In this case, they may not be appropriate algorithms for the samples numbered between 33 and 49 because all the variables were changed through the experiments and only the cutting parameters were used in the prediction of machine learning as shown in Figure 7.

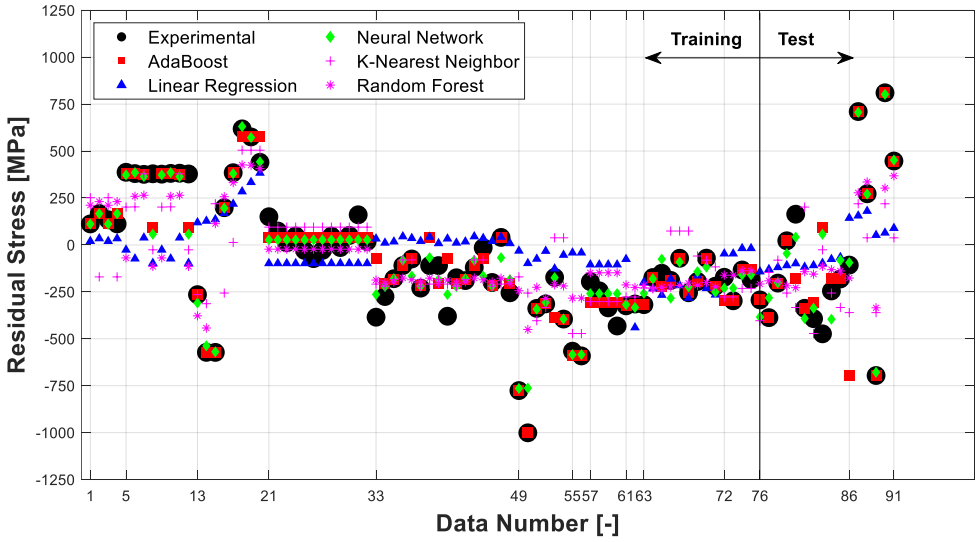

Figure 7. Experimental and predicted residual stresses in the turning of Ti6Al4V with only cutting parameters

Within the groups created from the datasets of Inconel 718 and Ti6Al4V materials, k-Nearest Neighbor and Random Forest algorithms gave similar errors. The maximum deviation between these two models was obtained in Group 2 with an MAE of approximately 25. However, the MAE of these models was still three to seven times greater than the one with the AdaBoost and Neural Network algorithms.

The performance of the employed five machine learning algorithms (Linear Regression, AdaBoost, Neural Network, Random Forest, k-Nearest Neighbor) was varied in the estimation of the residual stresses in the turning of Inconel 718 and Ti6Al4V. As highlighted before, while AdaBoost provided the best statistical scores for the Inconel 718 workpiece, the prediction accuracy was higher with Neural Network for Ti6Al4V. However, both of these algorithms still achieved to provide convincing statistical scores for two different datasets which shows the robustness of these algorithms in this study.

It is known that the use of datasets having a large sample size is a preferred situation when employing Machine Learning algorithms. However, data collection is not an easy task in the turning of difficult-to-cut materials (i.e., Nickel and Titanium alloys) due to the high cost of materials, experiments, and measurements. Although the residual stress predictions with the proposed machine learning models are remarkably in good agreement with the experimental data, the limitation of this research is that it has a relatively small sample size of the datasets for both workpiece materials. Several algorithms employed in this work (i.e., Linear Regression) were, thus, failed in the estimation of the surface residual stresses since the literature has a limited number of studies regarding the experimental investigation of machining induced residual stresses for these aerospace materials. Moreover, in most of the experimental studies used in this paper, all variable combinations were not tested, or an experimental design was not applied. Therefore, the machine learning models estimate the same residual stresses when the variables are grouped (Figure 5 and 7).

As presented in the introduction, ANN was also applied for the prediction of the residual stresses in the welding operation [25]. A hybrid ANN approach was also created for the prediction of the value of surface residual stresses in the face turning operation [22]. Even if the studies presented above fulfilled the aim of their own studies, they have some drawbacks. The first drawback is that there is no case study that was carried out to determine the optimal architecture of the created ANN in the studies presented above. In this sense, a more effective ANN architecture could be created which may improve the its performance in the prediction of the value of surface residual stresses in machining operations. Different iteration numbers of the ANN approaches were not also tested to obtain more reliable results in the prediction of machining induced residual stresses. In the proposed models described in the previous sections, a case study was carried out to determine the optimal structure for each learning algorithm. The second drawback of the existing research papers is that only one dataset has been used to evaluate the performance of the machine learning models. Unlike the presented work, the robustness of these studies has not been tested in the prediction of residual stresses.

4. Conclusions

This paper provides the experimental residual stresses measured by X-Ray Diffraction for various cutting and machine setup parameters used in the turning of aerospace materials. AdaBoost, Linear regression, Neural Network (ANN), K-nearest Neighbor, and Radom Forest machine learning models were used to predict the machining induced surface residual stresses for Inconel 718 and Ti6Al4V alloys. The performances of the models were then tested by calculating the Means Squared Error (MSE), Rooth Mean Square Error (RMSE), and Mean Absolute Error (MAE) as well as the R-squared. The datasets of these two workpieces were also grouped to clearly show the contribution of variables to the machining induced residual stresses. It was found that the AdaBoost gives the best agreement within the models used in this study for all Groups, and including the cooling and tool material type data into the machine learning models significantly increases the prediction accuracy of the models for the Inconel 718. On the other hand, Artificial Neural Network was the best fit in the prediction of surface residual stresses for all the group combinations of Ti6Al4V alloy. However, the MAE of the ANN was almost the same as the AdaBoost model when only cutting parameters were used in the analysis, and including one variable regarding the experimental setup reduced the MAE by approximately 50%. Therefore, the machine setup parameters are needed to accurately predict the machining induced residual stresses with Machine Learning models for Inconel 718 and Ti6Al4V materials. All the analyses showed that the AdaBoost and ANN algorithms can be used to estimate the residual stresses with an acceptable error range despite the small size of the datasets, and prevent the

cost of machining trials, experimental measurements and finite element software. Since the machine learning models with the optimum parameters determined in this study worked properly for both aerospace materials, the presented models can be extended to other types of workpieces. As a future work, the sample size of the datasets can also be increased using linear programming or heuristic models to employ the stacked ensemble models and deep learning algorithms in the prediction of surface residual stresses.

Acknowledgment

The authors gratefully acknowledge partial support of the Faculties of Engineering at Cankiri Karatekin University and Abdullah Gul University.

Contributions of the authors

Both authors developed the concept, designed the manuscript and created the original draft. Sinan Kesriklioglu collected and processed the datasets. Selim Buyrukoglu employed the machine learning models, and analyzed the data. Both authors discussed the results and approved the final version of the manuscript.

Conflict of Interest Statement

There is no conflict of interest between the authors.

Statement of Research and Publication Ethics

The authors declare that this study complies with Research and Publication Ethics.

References

[1] D. Ulutan and T. Ozel, "Machining induced surface integrity in titanium and nickel alloys: Areview", *International Journal of Machine Tools and MAnufacture.* 2011, doi: 10.1016/j.ijmachtools.2010.11.003.

[2] J. Holmberg, J. M. Rodríguez Prieto, J. Berglund, A. Sveboda, and P. Jonsén, "Experimental and PFEM-simulations of residual stresses from turning tests of a cylindrical Ti-6Al-4V shaft," 2018, doi: 10.1016/j.procir.2018.05.087.

[3] Y. Hua and Z. Liu, "Experimental investigation of principal residual stress and fatigue performance for turned nickel-based superalloy Inconel 718," *Materials (Basel).*, 2018, doi: 10.3390/ma11060879.

[4] F. Jafarian, H. Amirabadi, and J. Sadri, "Experimental measurement and optimization of tensile residual stress in turning process of Inconel718 superalloy," *Meas. J. Int. Meas. Confed.*, 2015, doi: 10.1016/j.measurement.2014.11.021.

[5] G. Kartheek, K. Srinivas, and C. Devaraj, "Optimization of Residual Stresses in Hard Turning of Super Alloy Inconel 718," 2018, doi: 10.1016/j.matpr.2017.12.029.

[6] K. Satyanarayana, A. V. Gopal, and N. Ravi, "Studies on surface integrity and its optimisation in turning Ti-6Al-4V," *Int. J. Precis. Technol.*, 2015, doi: 10.1504/ijptech.2015.073837.

[7] D. M. Madyira, R. F. Laubscher, N. Janse Van Rensburg, and P. F. J. Henning, "High speed machining induced residual stresses in Grade 5 titanium alloy," *Proc. Inst. Mech. Eng. Part L J. Mater. Des. Appl.*, 2013, doi: 10.1177/1464420712462319.

[8] Y. Ayed, G. Germain, A. P. Melsio, P. Kowalewski, and D. Locufier, "Impact of supply conditions of liquid nitrogen on tool wear and surface integrity when machining the Ti-6Al-4V titanium alloy," *Int. J. Adv. Manuf. Technol.*, 2017, doi: 10.1007/s00170-017-0604-7.

[9] A. Devillez, G. Le Coz, S. Dominiak, and D. Dudzinski, "Dry machining of Inconel 718, workpiece surface integrity," *J. Mater. Process. Technol.*, 2011, doi: 10.1016/j.jmatprotec.2011.04.011.

[10] G. Le Coz, R. Piquard, A. D'Acunto, D. Bouscaud, M. Fischer, and P. Laheurte, "Precision turning analysis of Ti-6Al-4V skin produced by selective laser melting using a design of experiment approach," *Int. J. Adv. Manuf. Technol.*, 2020, doi: 10.1007/s00170-020-05807-8.

[11] T. Özel and D. Ulutan, "Prediction of machining induced residual stresses in turning of titanium and nickel based alloys with experiments and finite element simulations," *CIRP Ann. - Manuf. Technol.*, 2012, doi: 10.1016/j.cirp.2012.03.100.

[12] A. Paranjpe and A, "RESIDUAL STRESSES IN MACHINED TITANIUM (Ti-6Al-4V) ALLOYS," *Statew. Agric. L. Use Baseline 2015*, 2015.

[13] A. R. C. Sharman, J. I. Hughes, and K. Ridgway, "An analysis of the residual stresses generated in Inconel 718™ when turning," *J. Mater. Process. Technol.*, 2006, doi: 10.1016/j.jmatprotec.2005.12.007.
[14] A. Simeone, T. Segreto, and R. Teti, "Residual stress condition monitoring via sensor fusion in turning of Inconel 718," 2013, doi: 10.1016/j.procir.2013.09.013.
[15] K. Jacobus, R. E. DeVor, and S. G. Kapoor, "Machining-induced residual stress: Experimentation and modeling," *J. Manuf. Sci. Eng. Trans. ASME*, 2000, doi: 10.1115/1.538906.
[16] S. Agrawal and S. S. Joshi, "Analytical modelling of residual stresses in orthogonal machining of AISI4340 steel," *J. Manuf. Process.*, 2013, doi: 10.1016/j.jmapro.2012.11.004.
[17] J. S. Y. Liang and J. C. Su, "Residual stress modeling in orthogonal machining," *CIRP Ann. - Manuf. Technol.*, 2007, doi: 10.1016/j.cirp.2007.05.018.
[18] D. Ulutan, B. Erdem Alaca, and I. Lazoglu, "Analytical modelling of residual stresses in machining," *J. Mater. Process. Technol.*, 2007, doi: 10.1016/j.jmatprotec.2006.09.032.
[19] J. C. Outeiro, J. C. Pina, R. M'Saoubi, F. Pusavec, and I. S. Jawahir, "Analysis of residual stresses induced by dry turning of difficult-to-machine materials," *CIRP Ann. - Manuf. Technol.*, 2008, doi: 10.1016/j.cirp.2008.03.076.
[20] N. K. Sahu and A. B. Andhare, "Prediction of residual stress using RSM during turning of Ti–6Al–4V with the 3D FEM assist and experiments," *SN Appl. Sci.*, 2019, doi: 10.1007/s42452-019-0809-5.
[21] M. Salio, T. Berruti, and G. De Poli, "Prediction of residual stress distribution after turning in turbine disks," *Int. J. Mech. Sci.*, 2006, doi: 10.1016/j.ijmecsci.2006.03.009.
[22] X. Ji, A. H. Shih, M. Rajora, Y. M. Shao, and S. Y. Liang, "A hybrid neural network for prediction of surface residual stress in MQL face turning," 2014, doi: 10.4028/www.scientific.net/AMM.633-634.574.
[23] D. Umbrello, G. Ambrogio, L. Filice, and R. Shivpuri, "An ANN approach for predicting subsurface residual stresses and the desired cutting conditions during hard turning," *J. Mater. Process. Technol.*, 2007, doi: 10.1016/j.jmatprotec.2007.01.016.
[24] M. Cheng *et al.*, "Prediction of surface residual stress in end milling with Gaussian process regression," *Meas. J. Int. Meas. Confed.*, 2021, doi: 10.1016/j.measurement.2021.109333.
[25] J. Mathew, J. Griffin, M. Alamaniotis, S. Kanarachos, and M. E. Fitzpatrick, "Prediction of welding residual stresses using machine learning: Comparison between neural networks and neuro-fuzzy systems," *Appl. Soft Comput. J.*, 2018, doi: 10.1016/j.asoc.2018.05.017.
[26] M. Ayeb, M. Frija, and R. Fathallah, "Prediction of residual stress profile and optimization of surface conditions induced by laser shock peening process using artificial neural networks," *Int. J. Adv. Manuf. Technol.*, 2019, doi: 10.1007/s00170-018-2883-z.
[27] O. Sagi and L. Rokach, "Ensemble learning: A survey," *Wiley Interdisciplinary Reviews: Data Mining and Knowledge Discovery*. 2018, doi: 10.1002/widm.1249.
[28] M. A. Ganaie, M. Hu, A. K. Malik, M. Tanveer, and P. N. Suganthan, "Ensemble deep learning: A review," Apr. 2021, doi: 10.48550/arxiv.2104.02395.
[29] I. Tsamardinos, E. Greasidou, and G. Borboudakis, "Bootstrapping the out-of-sample predictions for efficient and accurate cross-validation," *Mach. Learn.*, 2018, doi: 10.1007/s10994-018-5714-4.
[30] Y. Freund and R. E. Schapire, "Experiments with a New Boosting Algorithm," 1996, Accessed: Sep. 16, 2021. [Online]. Available: http://www.research.att.com/orgs/ssr/people/fyoav,schapireg/.
[31] H. Drucker, "Improving regressors using boosting techniques," *14th Int. Conf. Mach. Learn.*, 1997.
[32] M. Tranmer, J. Murphy, M. Elliot, and M. Pampaka, "Multiple Linear Regression (2 nd Edition)," 2020, Accessed: Sep. 16, 2021. [Online]. Available: https://hummedia.manchester.ac.uk/institutes/cmist/a.
[33] I. Riadi, A. Wirawan, and S. -, "Network Packet Classification using Neural Network based on Training Function and Hidden Layer Neuron Number Variation," *Int. J. Adv. Comput. Sci. Appl.*, 2017, doi: 10.14569/ijacsa.2017.080631.
[34] H. Balaga, N. Gupta, and D. N. Vishwakarma, "GA trained parallel hidden layered ANN based differential protection of three phase power transformer," *Int. J. Electr. Power Energy Syst.*, 2015, doi: 10.1016/j.ijepes.2014.11.028.
[35] G. E. Hinton, S. Osindero, and Y. W. Teh, "A fast learning algorithm for deep belief nets," *Neural Comput.*, 2006, doi: 10.1162/neco.2006.18.7.1527.

[36] S. Karsoliya, "Approximating Number of Hidden layer neurons in Multiple Hidden Layer BPNN Architecture," *Int. J. Eng. Trends Technol.*, 2012.
[37] S. Ray, "A Quick Review of Machine Learning Algorithms," 2019, doi: 10.1109/COMITCon.2019.8862451.
[38] Y. Liu, Y. Wang, and J. Zhang, "New machine learning algorithm: Random forest," 2012, doi: 10.1007/978-3-642-34062-8_32.
[39] D. Chicco, M. J. Warrens, and G. Jurman, "The coefficient of determination R-squared is more informative than SMAPE, MAE, MAPE, MSE and RMSE in regression analysis evaluation," *PeerJ Comput. Sci.*, 2021, doi: 10.7717/PEERJ-CS.623.
[40] X. Fu *et al.*, "Accuracy of X-ray diffraction measurement of residual stresses in shot peened titanium alloy samples," *Nondestruct. Test. Eval.*, 2019, doi: 10.1080/10589759.2019.1573239.
[41] M. R. Abonazel and O. M. Saber, "A comparative study of robust estimators for poisson regression model with outliers," *J. Stat. Appl. Probab.*, 2020, doi: 10.18576/jsap/090208.
[42] M. Kontaki, A. Gounaris, A. N. Papadopoulos, K. Tsichlas, and Y. Manolopoulos, "Efficient and flexible algorithms for monitoring distance-based outliers over data streams," *Inf. Syst.*, 2016, doi: 10.1016/j.is.2015.07.006.
[43] I. Oleaga, C. Pardo, J. J. Zulaika, and A. Bustillo, "A machine-learning based solution for chatter prediction in heavy-duty milling machines," *Meas. J. Int. Meas. Confed.*, 2018, doi: 10.1016/j.measurement.2018.06.028.
[44] A. Kortabarria, A. Madariaga, E. Fernandez, J.a. Esnaola, and P. J. Arrazola, "A comparative study of residual stress profiles on inconel 718 induced by dry face turning," 2011, doi: 10.1016/j.proeng.2011.11.105.
[45] A. B. Sadat, M. Y. Reddy, and B. P. Wang, "Plastic deformation analysis in machining of Inconel-718 nickel-base superalloy using both experimental and numerical methods," *Int. J. Mech. Sci.*, 1991, doi: 10.1016/0020-7403(91)90005-N.
[46] V. Veeranaath, R. K. Das, S. K. Rai, S. Singh, and P. Sharma, "Experimental Study and Optimization of Residual Stresses in Machining of Ti6Al4V Using Titanium and Multi-layered Inserts," 2020, doi: 10.1088/1757-899X/912/3/032028.
[47] J. D. P. Velásquez, A. Tidu, B. Bolle, P. Chevrier, and J. J. Fundenberger, "Sub-surface and surface analysis of high speed machined Ti-6Al-4V alloy," *Mater. Sci. Eng. A*, 2010, doi: 10.1016/j.msea.2009.12.018.
[48] S. Isakson, M. I. Sadik, A. Malakizadi, and P. Krajnik, "Effect of cryogenic cooling and tool wear on surface integrity of turned Ti-6Al-4V," 2018, doi: 10.1016/j.procir.2018.05.061.
[49] Z. Pan, S. Y. Liang, H. Garmestani, D. Shih, and E. Hoar, "Residual stress prediction based on MTS model during machining of Ti-6Al-4V," *Proc. Inst. Mech. Eng. Part C J. Mech. Eng. Sci.*, 2019, doi: 10.1177/0954406218805122.
[50] S. Joshi, A. Tewari, and S. S. Joshi, "Microstructural characterization of chip segmentation under different machining environments in orthogonal machining of Ti6Al4V," *J. Eng. Mater. Technol. Trans. ASME*, 2015, doi: 10.1115/1.4028841.

Appendix 1. Datasets of Inconel 718

Data #	Tool Material	Rake Angle	Coolant Type	Cutting Speed [m/min]	Feed (mm/rev)	Width of Cut [mm]	Surface Residual Stresses [MPa]	Reference
1	Coated	0	MWF	35	0.200	0.4	903	
2	Coated	0	MWF	44	0.100	0.3	609	
3	Coated	0	MWF	53	0.100	0.4	851	
4	Coated	0	MWF	35	0.150	0.3	775	
5	Coated	0	MWF	44	0.150	0.4	1020	[5]
6	Coated	0	MWF	35	0.100	0.2	562	
7	Coated	0	MWF	53	0.200	0.3	1125	
8	Coated	0	MWF	44	0.200	0.2	983	
9	Coated	0	MWF	53	0.150	0.2	1150	
10	Coated	Positive	DRY	50	0.075	0.2	371	
11	Coated	Positive	DRY	50	0.100	0.2	411	
12	Coated	Positive	DRY	50	0.125	0.2	444	
13	Coated	Positive	DRY	50	0.150	0.2	466	
14	Coated	Positive	DRY	60	0.075	0.2	354	
15	Coated	Positive	DRY	60	0.100	0.2	391	
16	Coated	Positive	DRY	60	0.125	0.2	385	
17	Coated	Positive	DRY	60	0.150	0.2	479	
18	Coated	Positive	DRY	70	0.075	0.2	321	[3]
19	Coated	Positive	DRY	70	0.100	0.2	366	
20	Coated	Positive	DRY	70	0.125	0.2	383	
21	Coated	Positive	DRY	70	0.150	0.2	437	
22	Coated	Positive	DRY	80	0.075	0.2	340	
23	Coated	Positive	DRY	80	0.100	0.2	377	
24	Coated	Positive	DRY	80	0.125	0.2	395	
25	Coated	Positive	DRY	80	0.150	0.2	459	
26	NA	0	DRY	30	0.150	0.15	376	
27	NA	0	DRY	30	0.250	0.15	575	
28	NA	0	DRY	70	0.150	0.15	589	[44]
29	NA	0	DRY	70	0.250	0.15	370	
30	Uncoated	Positive	MWF	60	0.015	0.15	153	
31	Uncoated	Positive	MWF	60	0.025	0.3	81	
32	Uncoated	Positive	MWF	60	0.035	0.45	196	
33	Uncoated	Positive	MWF	60	0.045	0.6	182	
34	Uncoated	Positive	MWF	80	0.015	0.15	243	
35	Uncoated	Positive	MWF	80	0.025	0.3	523	
36	Uncoated	Positive	MWF	80	0.035	0.45	514	
37	Uncoated	Positive	MWF	80	0.045	0.6	568	
38	Uncoated	Positive	MWF	100	0.025	0.15	230	
39	Uncoated	Positive	MWF	100	0.015	0.3	550	
40	Uncoated	Positive	MWF	100	0.045	0.45	177	
41	Uncoated	Positive	MWF	100	0.035	0.6	193	
42	Uncoated	Positive	MWF	120	0.025	0.15	203	
43	Uncoated	Positive	MWF	120	0.015	0.3	216	
44	Uncoated	Positive	MWF	120	0.045	0.45	211	
45	Uncoated	Positive	MWF	120	0.035	0.6	197	
46	Uncoated	Positive	MWF	60	0.045	0.15	188	[4]
47	Uncoated	Positive	MWF	60	0.035	0.3	175	
48	Uncoated	Positive	MWF	60	0.025	0.45	210	
49	Uncoated	Positive	MWF	60	0.015	0.6	221	
50	Uncoated	Positive	MWF	80	0.045	0.15	186	
51	Uncoated	Positive	MWF	80	0.035	0.3	206	
52	Uncoated	Positive	MWF	80	0.025	0.45	162	
53	Uncoated	Positive	MWF	80	0.015	0.6	196	
54	Uncoated	Positive	MWF	100	0.035	0.15	142	
55	Uncoated	Positive	MWF	100	0.045	0.3	167	
56	Uncoated	Positive	MWF	100	0.015	0.45	198	
57	Uncoated	Positive	MWF	100	0.025	0.6	231	
58	Uncoated	Positive	MWF	120	0.035	0.15	142	
59	Uncoated	Positive	MWF	120	0.045	0.3	179	
60	Uncoated	Positive	MWF	120	0.015	0.45	215	
61	Uncoated	Positive	MWF	120	0.025	0.6	217	

62	Uncoated	Positive	MWF	45	0.100	0.3	379	
63	Uncoated	Positive	MWF	45	0.125	0.3	182	
64	Uncoated	Positive	MWF	45	0.150	0.3	455	
65	Uncoated	Positive	MWF	50	0.100	0.3	309	
66	Uncoated	Positive	MWF	50	0.125	0.3	644	
67	Uncoated	Positive	MWF	50	0.150	0.3	767	
68	Uncoated	Positive	MWF	55	0.100	0.3	378	
69	Uncoated	Positive	MWF	55	0.125	0.3	662	
70	Uncoated	Positive	MWF	55	0.150	0.3	1009	[14]
71	Uncoated	Positive	MWF	80	0.150	0.3	1228	
72	Uncoated	Positive	MWF	80	0.300	0.3	1515	
73	Uncoated	Positive	MWF	100	0.150	0.3	1376	
74	Uncoated	Positive	MWF	100	0.300	0.3	1521	
75	Uncoated	Positive	DRY	80	0.150	0.3	1387	
76	Uncoated	Positive	DRY	80	0.300	0.3	1473	
77	Uncoated	Positive	DRY	100	0.150	0.3	1277	
78	Uncoated	Positive	DRY	100	0.300	0.3	1412	
79	Ceramic	Positive	MWF	12	0.028	3.24	608	
80	Ceramic	Positive	MWF	21	0.028	3.24	757	[45]
81	Ceramic	Positive	MWF	38	0.028	3.24	827	
82	Coated	Positive	MWF	40	0.150	0.25	611	
83	Coated	Positive	MWF	40	0.250	0.25	761	
84	Coated	Positive	MWF	80	0.150	0.25	244	
85	Coated	Positive	MWF	80	0.250	0.25	298	[13]
86	Coated	Positive	MWF	120	0.150	0.25	192	
87	Coated	Positive	MWF	120	0.250	0.25	326	
88	Uncoated	Positive	MWF	40	0.150	0.25	192	
89	Uncoated	Positive	MWF	40	0.250	0.25	259	
90	Ceramic	Positive	MWF	75	0.028	3.24	926	[45]
91	Ceramic	Positive	MWF	97	0.028	3.24	1039	
92	Coated	0	DRY	40	0.100	0.5	922	
93	Coated	0	DRY	60	0.100	0.5	720	
94	Coated	0	DRY	80	0.100	0.5	721	[9]
95	Coated	0	MWF	40	0.100	0.5	239	
96	Coated	0	MWF	60	0.100	0.5	227	
97	Coated	0	MWF	80	0.100	0.5	736	

Appendix 2. Datasets of Ti6Al4V

Data #	Tool Material	Rake Angle	Coolant Type	Cutting Speed [m/min]	Feed [mm/rev]	Width of Cut [mm]	Surface Residual Stress [MPa]	Reference
1	Uncoated	0	DRY	55	0.100	2	112	[11]
2	Uncoated	0	DRY	90	0.100	2	167	
3	Coated	0	DRY	55	0.100	2	134	
4	Coated	0	DRY	90	0.100	2	112	
5	Coated	0	DRY	50	0.100	1	387	[46]
6	Coated	0	DRY	50	0.200	2	380	
7	Coated	0	DRY	100	0.100	2	376	
8	Coated	0	DRY	100	0.200	1	379	
9	Coated	0	DRY	50	0.100	1	377	
10	Coated	0	DRY	50	0.200	2	381	
11	Coated	0	DRY	100	0.100	2	382	
12	Coated	0	DRY	100	0.200	1	378	
13	Ceramic	0	DRY	20	0.120	5	-265	[47]
14	Ceramic	0	DRY	40	0.120	5	-572	
15	Ceramic	0	DRY	60	0.120	5	-572	
16	Ceramic	0	DRY	140	0.120	5	198	
17	Ceramic	0	DRY	260	0.120	5	385	
18	Ceramic	0	DRY	420	0.120	5	618	
19	Ceramic	0	DRY	540	0.120	5	575	
20	Ceramic	0	DRY	660	0.120	5	440	
21	Uncoated	Negative	DRY	75	0.200	1.2	150	[12]
22	Uncoated	Negative	MQL	75	0.200	1.2	74	
23	Uncoated	Negative	MWF	75	0.200	1.2	11	
24	Uncoated	Negative	DRY	75	0.200	1.2	48	
25	Uncoated	Negative	MQL	75	0.200	1.2	-29	
26	Uncoated	Negative	MWF	75	0.200	1.2	-73	
27	Coated	Negative	DRY	75	0.200	1.2	-29	
28	Coated	Negative	MQL	75	0.200	1.2	47	
29	Coated	Negative	MWF	75	0.200	1.2	-14	
30	Coated	Negative	DRY	75	0.200	1.2	51	
31	Coated	Negative	MQL	75	0.200	1.2	161	
32	Coated	Negative	MWF	75	0.200	1.2	18	
33	Uncoated	0	DRY	100	0.012	0.06	-385	[10]
34	Uncoated	Positive	DRY	40	0.012	0.12	-275	
35	Uncoated	Positive	DRY	40	0.002	0.06	-180	
36	Uncoated	0	DRY	100	0.002	0.12	-110	
37	Uncoated	Positive	DRY	100	0.012	0.12	-75	
38	Uncoated	0	DRY	40	0.002	0.12	-230	
39	Uncoated	Positive	DRY	100	0.002	0.06	-110	
40	Uncoated	0	DRY	40	0.012	0.06	-110	
41	Uncoated	0	DRY	100	0.012	0.06	-380	
42	Uncoated	Positive	DRY	40	0.012	0.12	-175	
43	Uncoated	Positive	DRY	40	0.002	0.06	-190	
44	Uncoated	Positive	DRY	100	0.002	0.12	-120	
45	Uncoated	Positive	DRY	100	0.012	0.12	-15	
46	Uncoated	0	DRY	40	0.002	0.12	-200	
47	Uncoated	Positive	DRY	100	0.002	0.06	40	
48	Uncoated	0	DRY	40	0.012	0.06	-255	
49	Coated	Positive	DRY	90	0.100	0.50	-776	[20]
50	Coated	Positive	DRY	151	0.200	0.50	-1001	
51	Coated	Positive	DRY	70	0.150	0.75	-338	
52	Coated	Positive	DRY	171	0.150	0.75	-314	
53	Coated	Positive	DRY	121	0.230	0.75	-173	
54	Coated	Positive	DRY	121	0.150	0.75	-395	
55	Uncoated	NA	MWF	70	0.150	1.5	-566	[48]
56	Uncoated	NA	CRYO	70	0.150	1.5	-591	
57	Uncoated	Positive	DRY	80	0.200	1	-196	[8]
58	Uncoated	Positive	MWF	80	0.200	1	-245	
59	Uncoated	Positive	CRYO	80	0.200	1	-335	
60	Uncoated	Positive	CRYO	80	0.200	1	-432	
61	NA	0	NA	26	0.100	0.1	-325	[49]
62	NA	0	NA	26	0.500	0.1	-315	

63	Coated	Negative	DRY	45	0.250	0.25	-318	
64	Coated	Negative	DRY	45	0.300	0.5	-174	
65	Coated	Negative	DRY	45	0.350	0.75	-151	
66	Coated	Negative	DRY	60	0.250	0.5	-189	
67	Coated	Negative	DRY	60	0.300	0.75	-71	[6]
68	Coated	Negative	DRY	60	0.350	0.25	-255	
69	Coated	Negative	DRY	75	0.250	0.75	-195	
70	Coated	Negative	DRY	75	0.300	0.25	-71	
71	Coated	Negative	DRY	75	0.350	0.5	-220	
72	Coated	Positive	DRY	23	0.110	1	-172	
73	Coated	Positive	CRYO	23	0.110	1	-298	[50]
74	Coated	Positive	DRY	92	0.110	1	-134	
75	Coated	Positive	CRYO	92	0.110	1	-184	
76	Uncoated	Positive	MWF	70	0.200	0.25	-293	
77	Uncoated	Positive	MWF	100	0.200	0.25	-387	
78	Uncoated	Positive	MWF	125	0.200	0.25	-203	
79	Uncoated	Positive	MWF	150	0.200	0.25	22	
80	Uncoated	Positive	MWF	175	0.200	0.25	164	
81	Uncoated	Positive	MWF	50	0.200	1	-338	[7]
82	Uncoated	Positive	MWF	70	0.200	1	-393	
83	Uncoated	Positive	MWF	100	0.200	1	-474	
84	Uncoated	Positive	MWF	150	0.200	1	-245	
85	Uncoated	Positive	MWF	175	0.200	1	-181	
86	Coated	Negative	DRY	30	0.050	4	-107	
87	Coated	Negative	DRY	60	0.050	4	710	
88	Coated	Negative	DRY	120	0.050	4	272	
89	Coated	Negative	DRY	30	0.150	4	-696	[2]
90	Coated	Negative	DRY	60	0.150	4	810	
91	Coated	Negative	DRY	120	0.150	4	447	